Available online at www.sciencedirect.com
SCIENCE DIRECT®
ELSEVIER
Nuclear Instruments and Methods in Physics Research B 202 (2003) 100–106
NIM B
Beam Interactions with Materials & Atoms
www.elsevier.com/locate/nimb

Modeling SiC swelling under irradiation: Influence of amorphization

Antonino Romano [a], Marjorie Bertolus [a,b,*], Mireille Defranceschi [c], Sidney Yip [a]

[a] *Department of Nuclear Engineering, Massachusetts Institute of Technology, 77 Massachusetts Avenue, Cambridge, MA 02139, USA*
[b] *CEA Cadarache, Département d'Etudes des Déchets, SEP/LCC, Bâtiment 332, 13108 Saint-Paul-lez-Durance, France*
[c] *CEA Saclay, Direction de l'Energie Nucléaire, DSOE/RB, Bâtiment 121, 91191 Gif-sur-Yvette, France*

Abstract

Irradiation-induced swelling of SiC is investigated using a molecular dynamics simulation-based methodology. To mimic the effect of heavy ion irradiation extended amorphous areas of various sizes are introduced in a crystalline SiC sample, and the resulting configurations are relaxed using molecular dynamics at constant pressure. Simulation results compare very well with data from existing ion implantation experiments. Analysis of the relaxed configurations shows very clearly that SiC swelling does not scale linearly with the amorphous fraction introduced. Two swelling regimes are observed depending on the size of the initial amorphous area: for small amorphous zones swelling scales like the amorphous fraction to the power 2/3, while for larger areas it scales like the amorphous fraction to the powers 2/3 and 4/3. Similar dependences on the amorphous fraction are obtained for the number of homonuclear bonds present in the initial amorphous volume and for the number of short bonds created at the interface between crystalline and amorphous phases. Both the structural and chemical disorders introduced therefore seem to be driving forces for the material swelling. This is confirmed by the evolution of these disorders after relaxation: comparison of the initial and relaxed configurations shows that swelling is accompanied by a decrease of the number of short bonds and an increase of the structural and chemical disorders.

PACS: 61.80.Az; 61.82.Fk; 64.60.Cn
Keywords: SiC; Irradiation-induced swelling; Amorphization; Classical molecular dynamics simulations

1. Introduction

The evolution of structural and mechanical properties of materials in high-radiation environment, and in particular irradiation-induced swelling, is an important issue in nuclear applications. Numerous experimental studies of volume changes in ceramics under irradiation have been published over the years [1], but there are no theoretical studies of the irradiation-induced swelling and the atomic-scale mechanisms behind it are not well understood. A linear behavior of swelling versus the fraction of amorphous material is often assumed for various materials [1]. Experimental ion

* Corresponding author. Address: Department of Nuclear Engineering, Massachusetts Institute of Technology, 77 Massachusetts Avenue, Cambridge, MA 02139, USA. Tel.: +1-617-253-1655; fax: +1-617-258-8863.
E-mail address: marj@mit.edu (M. Bertolus).

0168-583X/02/$ - see front matter
doi:10.1016/S0168-583X(02)01840-2

implantation studies [2–4] and Monte Carlo binary collision simulations [5] on SiC, however, tend to show that the swelling of this material under irradiation is a much more complex phenomenon, not completely understood and worth investigating using both theoretical and numerical approaches.

SiC is a promising material for nuclear applications [6,7], as well as relatively simple to model thanks to the availability of successful interatomic potentials which enable the accurate study of defects in SiC using classical molecular dynamics simulations [8–10]. We have therefore chosen to start investigating the mechanisms of irradiation-induced swelling on this material. We address here the influence of extended disordered or amorphous zones on SiC swelling using an original molecular dynamics simulation-based methodology. In particular, the structural and chemical disorders induced are investigated to get further insight on the driving forces for swelling.

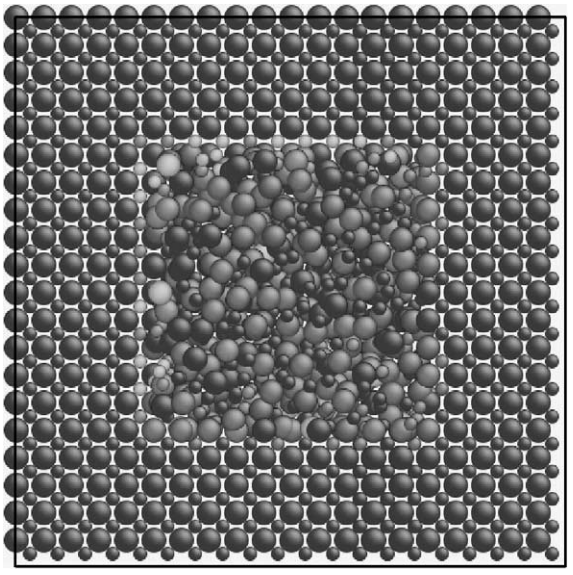

Fig. 1. (1 0 0) section at midplane of the initial composite sample for an initial amorphous fraction equal to 12.25%. Large and small spheres represent Si and C atoms, respectively.

2. Simulation and method

Heavy ion irradiation is assumed to affect the material in two steps: (a) creation of local atomic disorder, (b) induced swelling. Modeling of these two steps is as follows. First, in order to mimic the local amorphization induced by irradiation a composite sample is constructed by substituting a cubic area at the center of a crystalline SiC supercell with a disordered zone. The total simulation box has initial dimension $V_0 = 10a_0 \times 10a_0 \times 10a_0$, where a_0 is the SiC lattice parameter (4.36 Å), and consists of a constant number of atoms (8000). The disordered zone is obtained by quenching a SiC liquid at constant volume and has the same density as the crystalline phase. Various fractions f_a of initial amorphous material from 0.65% to 72.6% are inserted. A section of the composite sample constructed for an initial amorphous fraction equal to 12.25% is represented in Fig. 1. Second, swelling is obtained by letting these initial configurations relax using classical molecular dynamics. All the molecular dynamics simulations have been performed using an MIT in-house code [8] with constant pressure and temperature (NPT ensemble) and periodic boundary conditions. The interactions between atoms are described using a modified Tersoff interatomic potential as described in [8]. Relaxation times are approximately 400 ps.

We then analyze the initial and relaxed configurations, in particular the volume change $\Delta V/V_0 = (V_{\text{final}} - V_0)/V_0$, the distribution of interatomic distances, and the number of homonuclear bonds relatively to the initial amorphous fraction introduced. In addition, the AtomEye software [11] is used to visualize and determine the coordination number of atoms in the samples. Initial configurations can be seen as the result of the disorder created by the ion bombardment or disintegrations before relaxation has occurred. It is therefore reasonable to assume that these configurations have some physical meaning and contain elements that govern relaxation. Analysis of both initial and relaxed configurations can then bring insight on the driving forces for the observed swelling.

3. Results and discussion

3.1. Variation of volume after relaxation

Fig. 2 shows the relative volume change $\Delta V/V_0$ as a function of the initial amorphous fraction (a) in our molecular dynamics simulations, (b) in the ion implantation experiments by Bolse et al. [3], (c) in the ion implantation experiments by Nipoti et al. [4]. On the experimental curves the amount of disorder is expressed either as the integral of displaced atoms [3] or as the areal density of amorphous material [4]. These parameters are determined from Rutherford backscattering spectra using various dechanneling approximations, and are proportional to the total amount of disorder in the sample [3,4], therefore to the fraction of amorphous material considered in our simulation. It can be seen from this figure that $\Delta V/V_0$ does not scale linearly with the amorphous fraction, and that the molecular dynamics results compare very well with the experimental curves by Bolse and Nipoti. In addition, for the completely amorphous system ($f_a = 1$) the swelling obtained is 8.2%, as in the molecular dynamics simulations from Gao et al. [12]. Our model therefore seems reasonable. Two different regimes are observed in our data as well as in the experimental curves: for small initial amorphous zones (up to 12.25% in our model) the volume change can be fitted perfectly by $\Delta V/V_0 = \alpha_1 x^{2/3}$, while for larger initial amorphous areas $\Delta V/V_0 = \beta_1 + \beta_2 x^{2/3} + \beta_3 x^{4/3}$, where x is the initial amorphous fraction in our simulations or an equivalent parameter (integral of displaced atoms or areal density of amorphous material) in the experiments. Table 1 lists the values of the α_1, β_1, β_2 and β_3 parameters for the three curves. To get further insight on this scaling we have analyzed the structural and chemical disorders in our samples before and after relaxation.

3.2. Structural disorder: overall interatomic distance distribution

Fig. 3 shows the overall interatomic distance distributions before and after relaxation for two initial amorphous fractions: (a) 2.475% and (b) 50.9%, as well as for an amorphous SiC sample.

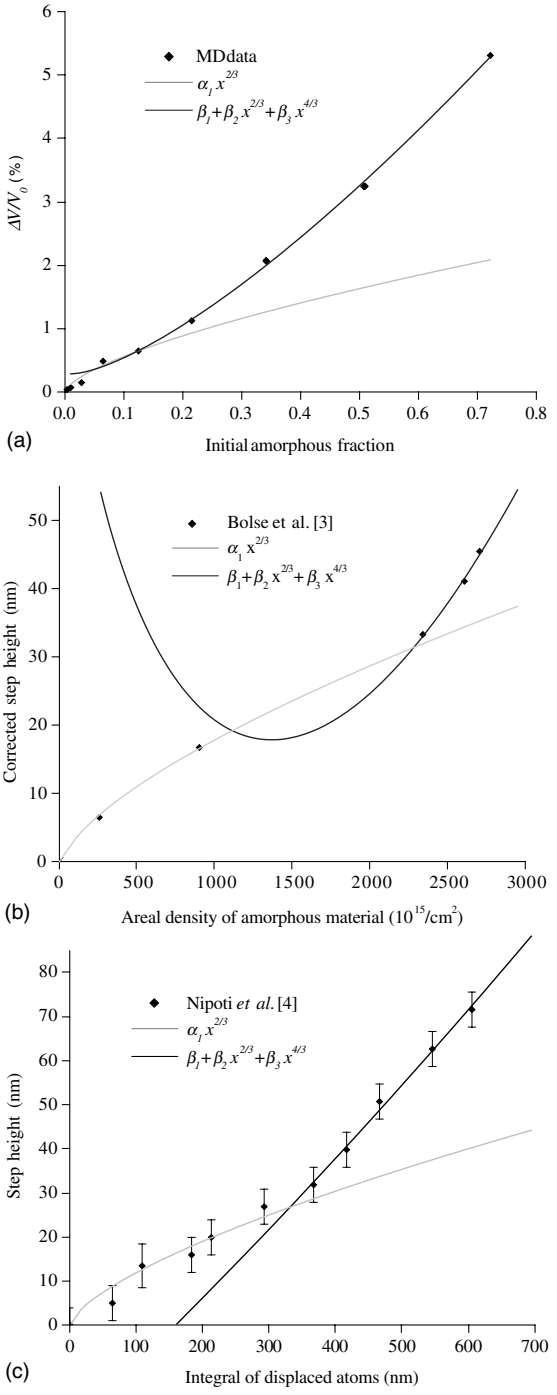

Fig. 2. Relative volume change $\Delta V/V_0$ as a function of the initial amorphous fraction (a) in our molecular dynamics simulations, (b) in the ion implantation experiments by Bolse et al. [3], (c) in the ion implantation experiments by Nipoti et al. [4].

Table 1
Values of the α_1, β_1, β_2 and β_3 parameters in our molecular dynamics simulations, in the experiments by Bolse et al. [3], and the experiments by Nipoti et al. [4]

Results	α_1	β_1	β_2	β_3
MD	2.495	0.267	−0.671	8.576
Bolse et al. [3]	0.165	97.537	−1.188	0.054
Nipoti et al. [4]	0.517	−26.156	0.51	0.011

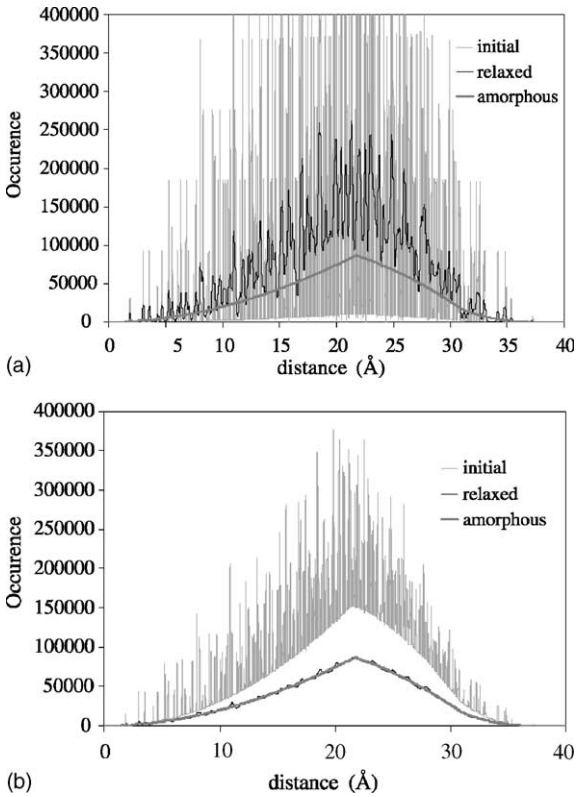

Fig. 3. Overall interatomic distance distributions before and after relaxation for two initial amorphous fractions: (a) 2.475 and (b) 50.9%, as well as for an amorphous SiC sample.

Before relaxation, the juxtaposition of crystalline and amorphous fractions is clearly visible on the histograms: the crystalline peaks are still very sharp but an offset is observed. After relaxation, a significant decrease of intensity of the crystalline peaks can be seen, and the distance distributions get closer to the distance distribution observed for a completely amorphous sample. Moreover, as the initial amorphous fraction increases the distance distributions after relaxation become very similar to the distribution for the pure amorphous sample, as can be seen in Fig. 3(b). Structural disorder therefore increases during relaxation. This is confirmed by comparing the initial and relaxed configurations themselves. For all initial amorphous fractions the disordered area has extended during relaxation. In addition, in the remaining crystalline areas point defects are observed, and many atoms are slightly displaced from their original lattice

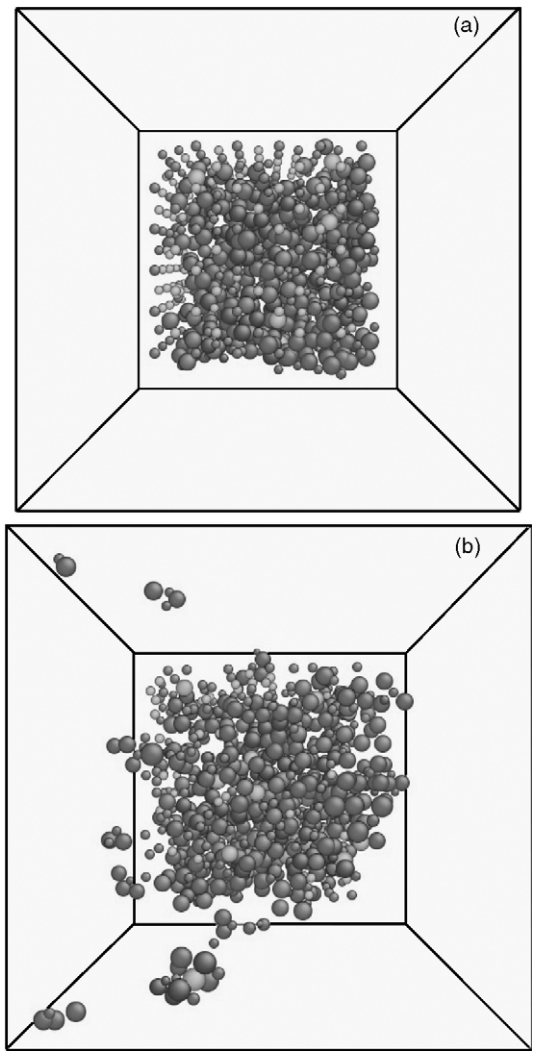

Fig. 4. Disordered atoms, i.e. atoms with a coordination number different from 4, in the initial (a) and relaxed configurations (b) for an initial amorphous fraction of 12.25%.

sites. To illustrate this we have represented in Fig. 4 the "disordered" atoms, i.e. the atoms with a coordination number different from 4 as calculated by the AtomEye visualization software, in the initial and relaxed configurations for an initial amorphous fraction of 12.25%. An increase of the structural disorder is clearly visible.

3.3. Structural disorder: presence of short bonds at the interface

The analysis of the initial distance distributions also shows the presence of bonds shorter than 1.3 Å, which corresponds to the shortest C–C distance found in the amorphous sample. Since these bond distances are shorter than any interatomic distances found in either the crystalline or the completely amorphous samples they can only be found at the interface between the two phases and have their origin in the juxtaposition of the two phases when we build our composite sample. It is reasonable to assume that this interface is physically important although it is built artificially in our model. We have therefore carried out a detailed analysis of these short bonds to determine more precisely their influence on swelling. The number of short bonds n_s created as a function of the amorphous fraction is shown in Fig. 5. The points obtained can be fitted very well with the expression: $n_s = \alpha_1 f_a^{2/3}$ with $\alpha_1 = 893.6$. We see that the number of short bonds scales like the initial amorphous fraction to the power 2/3. This can be interpreted as follows. We consider the interface between the crystalline and amorphous phase as the small volume containing the outer atom layer of the amorphous zone and the first layer of the crystal. If V_0 is the total volume of the simulation box and f_a the initial amorphous fraction, the interface area A_i can be expressed as $6\ (f_a V_0)^{2/3}$. The number of atoms at the interface n_i is equal to $dA_i w_i$, where d is the density of the initial amorphous phase (same as crystalline by construction), and w_i the interface width. Using the previous expression for A_i, one finds

$$n_i = 6 d w_i V_0^{2/3} f_a^{2/3}.$$

The density d and the total volume V_0 are constant, and our construction of the interface induces that the interface width w_i remains approximately constant for the various amorphous fractions considered. Therefore, n_i is proportional to $f_a^{2/3}$. Since n_s also scales like the initial amorphous fraction to the power 2/3, it is reasonable to assume that the number of short bonds is proportional to the number of atoms at the interface.

A similar dependence on $f_a^{2/3}$ is observed for the volume change, especially in the first regime, so the disorder created at the interface seems to be part of the driving force for swelling. This is confirmed by the decrease of the number of short bond distances observed after relaxation for all amorphous zone

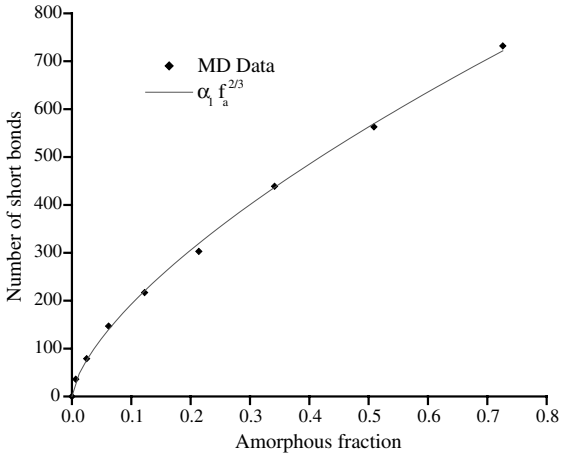

Fig. 5. Number of short bonds created as a function of the amorphous fraction.

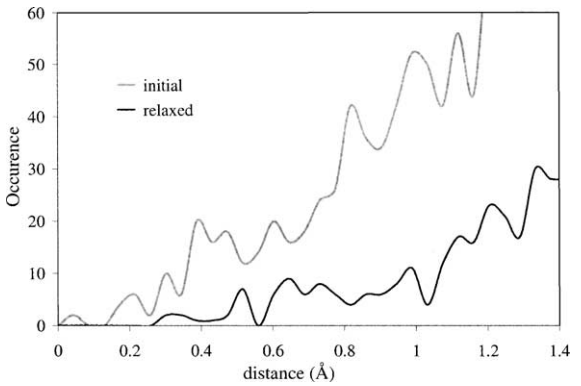

Fig. 6. Number of short bonds before and after relaxation for an initial amorphous fraction equal to 50.9%.

sizes, as shown in Fig. 6 for an initial amorphous fraction equal to 50.9%. This decrease is probably due to the relaxation of stresses generated in the material by these short bonds. We are currently carrying out further simulations to study the stresses present in the material, and in particular near the interface.

3.4. Chemical disorder

We have also analyzed the chemical disorder introduced by the amorphous zones and its evolution after relaxation. We have calculated the numbers of C and Si atoms of the initial configurations forming at least one homonuclear bond C–C or Si–Si: n^0_{Ch} and n^0_{Sih}, respectively. The variation of n^0_{Ch} and n^0_{Sih} relatively to the initial amorphous fraction is represented in Fig. 7. Both n^0_{Ch} and n^0_{Sih} vary like $\beta_1 f_{\mathrm{a}}^{2/3} + \beta_2 f_{\mathrm{a}}^{4/3}$ with $\beta_1 = 91.24$, $\beta_2 = 5.43$ for C and $\beta_1 = 82.8$, $\beta_2 = 5.06$ for Si. Again, a similar scaling on f_{a} as for $\Delta V/V_0$ is observed, so that the chemical disorder also seems to have an influence on swelling. In addition, the analysis of the relaxed configurations shows that the number of C and Si atoms forming at least one homonuclear bond increases after relaxation for all initial amorphous fractions. Therefore, an increase of the chemical disorder is observed after relaxation. The slight increase of the number of C with four C neighbors also shows the onset of a phase segregation between C and SiC.

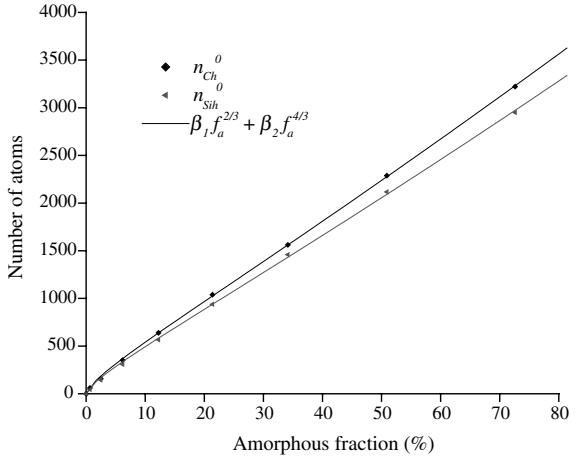

Fig. 7. Variation of n^0_{Ch} and n^0_{Sih} relative to the initial amorphous fraction.

4. Conclusion

We have investigated the influence of the introduction of extended amorphous areas on SiC swelling using classical molecular dynamics. The results of our simulations compare very well with results of existing ion implantation experiments and show very clearly that SiC swelling does not scale linearly with the amorphous fraction introduced. Two swelling regimes are observed relatively to the size of the amorphous area: for small initial amorphous zones swelling scales like the amorphous fraction to the power 2/3, while for larger initial amorphous areas it scales like the amorphous fraction to the powers 2/3 and 4/3. Similar dependences on the amorphous fraction are obtained for the number of homonuclear bonds present in the initial amorphous volume and for the number of short bonds created at the interface between crystalline and amorphous phases. Both the structural and chemical disorders introduced therefore seem to be driving forces for the material swelling. This is confirmed by the evolution of these disorders after relaxation: comparison of the initial and relaxed configurations shows that swelling is accompanied by a decrease of the number of short bonds and an increase of the structural and chemical disorders. More study is needed to determine the exact mechanisms in the two different regimes and the relationship between the two types of disorder. Calculation of stresses present in the material and in particular at the interface between amorphous and crystalline areas and their evolution during relaxation should bring more insight on the atomic-scale mechanisms of swelling.

References

[1] W.J. Weber, R.C. Ewing, C.R.A. Catlow, T. Diaz de la Rubia, L.W. Hobbs, C. Kinoshita, H. Matzke, A.T. Motta, M. Nastasi, E.K.H. Salje, E.R. Vance, S.J. Zinkle, J. Mater. Res. 13 (1998) 1434.

[2] C.J. McHargue, J.M. Williams, Nucl. Instr. and Meth. B 80–81 (1993) 889.
[3] W. Bolse, J. Conrad, T. Rödle, T. Weber, Surf. Coat. Technol. 74–75 (1995) 927.
[4] R. Nipoti, E. Albertazzi, M. Bianconi, R. Lotti, G. Lulli, M. Cervera, A. Carnera, Appl. Phys. Lett. 70 (1997) 3425.
[5] G. Lulli, E. Albertazzi, M. Bianconi, R. Nipoti, Nucl. Instr. and Meth. B 148 (1999) 573.
[6] P. Fenici, A.J.F. Rebolo, R.H. Jones, A. Kohyama, L.L. Snead, J. Nucl. Mater. 258 (1998) 215.
[7] R.A. Verrall, M.D. Vlajic, V.D. Krstic, J. Nucl. Mater. 274 (1999) 54.
[8] J. Li, L.J. Porter, S. Yip, J. Nucl. Mater. 246 (1997) 53.
[9] R. Devanathan, W.J. Weber, T. Diaz de la Rubia, Nucl. Instr. and Meth. B 141 (1998) 118.
[10] J.M. Perlado, L. Malerba, A. Sanchez-Rubio, T. Diaz de la Rubia, J. Nucl. Mater. 276 (2000) 235.
[11] J. Li, private communication. Available from <http://long-march.mit.edu/liju99/Graphics/A>.
[12] F. Gao, W.J. Weber, R. Devanathan, Nucl. Instr. and Meth. B 191 (2002) 487.